Journal of Applied Polymer Science

Influence of the Processing Parameters and Composition on the Thermal Stability of PLA/Nanoclay Bio-Nanocomposites

Maider Iturrondobeitia,[1] Ana Okariz,[1] Teresa Guraya,[1] Ane-Miren Zaldua,[2] Julen Ibarretxe[3]
[1]University of the Basque Country, Rafael Moreno Pitxitxi 3, 48013 Bilbao, Spain
[2]Materials Department-LEARTIKER, Lea Artibai Ikastetxea S. Coop., 48270 Markina-Xemein, Spain
[3]University of the Basque Country, Rafael Moreno Pitxitxi 2, 48013 Bilbao, Spain
Correspondence to: J. Ibarretxe (E-mail: julen.ibarretxe@ehu.es)

ABSTRACT: Poly(lactic acid) (PLA) is one the most promising bio-based and biodegradable polymer. However, its low thermal stability limits the range of applications and complicates its transformation via the most industrial common processes. The novelty of this work is studying the thermal stability of PLA and PLA/clay nanocomposites during use, as a function of the composition and using a wide range of extrusion and injection moulding processing parameters. To improve the thermal stability of the PLA, laminar silicates containing different organomodifications have been added (Cloisite 20A and Cloisite 30B). The results show that the processing conditions and composition define the morphology of the bio-nanocomposites, which plays key role in defining final thermal properties of the material. In general, clays improve the thermal stability of the processed material, increasing the degradation temperature and decreasing the degradation rate under a wide range of processing conditions. © 2014 Wiley Periodicals, Inc. J. Appl. Polym. Sci. **2014**, *131*, 40747.

KEYWORDS: biopolymers and renewable polymers; clay; extrusion; morphology; thermal properties

Received 23 November 2013; accepted 20 March 2014
DOI: 10.1002/app.40747

INTRODUCTION

Poly(lactic acid) or PLA is one the most commercially important biodegradable and biocompatible polymers.[1] It can be derived from renewable sources, it is environmentally friendly and it exhibits a combination of physical properties that meet the requirements for many applications, notably for packaging. All these features make PLA an attractive alternative for synthetic plastic materials which degrade too slowly and have their origin in petrochemical resources. However, the use of PLA in other industries (like the automotive sector) is limited mainly due to its low medium- to long-term stability. PLA can undergo biodegradation under certain conditions; 70% humidity, presence of microorganisms and temperatures around 60°C or higher.[2] Hence, when working at room temperature and in non aqueous conditions biodegradation is not expected to occur and it will not be considered here.

To improve the mechanical and thermal properties of PLA and limit its degradation, different polymer/silicate nanocomposites have been explored: montmorillonites and fluorohectorite clays or organomodified clays have been blended with the polymer. According to Okamoto and coworker,[3] the combination of polymer and clays at the nanoscale often results in remarkably improved mechanical and functional properties with respect to the neat polymers or conventional composites (either micro- or macrocomposites). The observed changes can be ascribed to an efficient interfacial interaction between matrices and organically modified layered silicates as recently shown by Wei et al., Fukushima et al., or Najafi et al. among others.[4–13] Regarding the medium- to long-term stability of this type of nanocomposites, it has been shown that clays act as a barrier towards water absorption and therefore the chances of observing biodegradation at room temperature are further reduced.[2,14] Thus, this work will be focused solely on the study of the thermal stability of PLA/clay nanocomposites as a function of the processing conditions.

Regarding the controversy on the risks of the use of nanoparticles in general, it must be pointed out that the safety of clays in food, cosmetic, and medical applications is widely supported in literature.[15–17]

Nowadays, the main transformation technologies for PLA are based on melt processing, the main problem of which is the low thermal stability of PLA and the resulting degradation of the polymer.[18,19] It has been widely reported that the presence of moisture, lactic acid, and metal catalyst residues, accompanied by high temperatures and shear favor the degradation of PLA.[2,20–23] The thermal degradation of PLA and its layered

Table I. Characteristics of the Studied Clays

Commercial name	Clay type	Interlayer cations	Interlayer distance (Å)	Dimensions (μm)	Weight loss ignition (%)
Cloisite 30B	MMT	$CH_3—N^+(CH_2CH_2OH)_2—T$	18.5	10% <2 50% <6 90% <13	30
Cloisite 20A	MMT	$CH_3—N^+(CH_3)—HT$	24.2	10% <2 50% <6 90% <13	38

composites are very complex and several mechanisms have been postulated by McNeill and Leiper and Kopinke et al. which include: random chain scission, intramolecular transesterification, intermolecular transesterification, hydrolysis, pyrolytic elimination, and radical degradation.[24–30]

The aim of this work is to study the thermal stability of PLA and PLA-based layered composites for a wide range of extrusion and injection moulding processing conditions. Thermal stability studies have already been reported, but the novelty of this work is the addition of a wide range of industrial processing conditions to such a study, and the analysis of the thermal stability of the resulting materials, as a function of the processing conditions and composition. To broaden the applicability of PLA to new areas such as the automotive or electrical industry, its properties, including the thermal stability, need to be improved. The addition of specific reinforcements via extrusion could provide the sought improvement. Also, depending on the chosen reinforcement, the processing parameters required to obtain an optimum composite or nanocomposites will vary.

Here, first the degradation during the processing will be studied. Then, also the thermal stability of the final material will be analyzed. Finally, to find the optimal processing conditions in terms of thermal stability of the final product, the relationship between processing conditions, composition, and obtained properties will be analyzed.

EXPERIMENTAL

Materials and Processing

Natureworks® LLC polymer grade 3051D PLA was provided by Cargill-Dow. The material was received in pellets having a melt flow index of 9 g 10 min^{-1} (190°C and 2.16 kg). Organically treated montmorillonite Cloisite® 30B and 20A from Southern Clay Products (Gonzales, TX) were used as reinforcement (see Table I).

The amount of clays used to prepare the nanocomposites was set at 5 wt %. According to literature the effect of clays varies with their concentration, which typically can be varied from 0.5 wt % up to 10 wt %. An intermediate value of 5 wt % was selected to make sure that improvements in thermal stability could be measured.[12] The PLA/clay nanocomposite testing specimens were prepared by first mixing the materials by extrusion and then injection moulding them. The design of experiments was done using a general full factorial design (3^2 2^1), where the selected factors were the composition, extrusion screw speed, both studied at three different levels and the injection moulding speed studied at two levels.

The PLA/clay samples were prepared in a Brabender Plasticorder DSE 20/40D co-rotating twin-screw extruder (Figure 1). The production rate was 1.5 kg h^{-1}, where PLA and nanoclays were fed gravimetrically. The configuration of the screws was

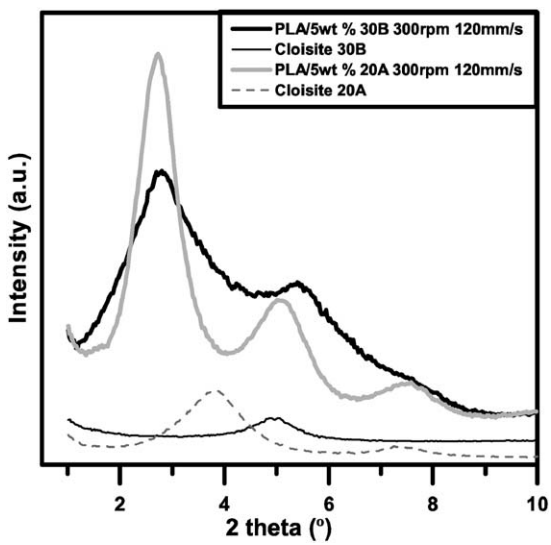

Figure 1. XRD diffraction patterns of Cloisite 20A and 30B organo-clays and of the PLA/5 wt % Cloisite 20A and Cloisite 30B nanocomposites, both processed at 300 rpm extrusion speed and 120 mm s^{-1} injection molding speed.

Table II. Processing Conditions Used for the Neat PLA, and the Two Composites (PLA/Cloisite 30B and PLA/Cloisite 20A)

Extrusion screw speed (rpm)	Injection speed (mm s^{-1})
120	120
120	240
300	120
300	240
650	120
650	240

specially designed for an optimal mixture between the matrix and nano-additives and the relation L/D for the screws was 40. Before processing, the PLA was dried for 4 h at 80°C and the clay for 12 h at 80°C. The blending temperature—which directly affects the degradation of the matrix and decomposition of the organic modification of the clay—was set at 190°C as specified in the material data sheet of the PLA. The screw speed, parameter that favors the shear induced delamination of the clays, was set at a low (120 rpm), medium (300 rpm), or high (650 rpm) speed.

The samples were also pre-dried for injection moulding for 4 h at 80°C, and A type specimens were injection moulded according to ISO 527 in a Sandretto OTTO 150 Tn injection moulding machine. During this processing step, the temperature of the melt was set at 190°C, the mould temperature at 30°C and the injection pressure was kept constant at 600 bar. To study the effect of the possible anisotropic orientation of the clay platelets through the polymeric matrix the specimens were injection moulded at two very different injection speeds: low (120 mm s^{-1}) and high (240 mm s^{-1}).

As a reference of the behavior of the base polymer used for the composites, the neat PLA was also extruded and then injected to make it undergo the same extrusion and injection processes as the nanocomposites. Table II summarizes the processing conditions used to prepare the samples. The six combinations of processing conditions presented in that table were used for all three materials (PLA, PLA/Cloisite 30B and PLA/Cloisite 20A), generating a set of 18 different samples.

Characterization Techniques

Molecular Weight. Molecular weight measurements were performed by gel permeation chromatography (GPC). The samples were injected in a Perkin Elmer Series 200 system, running at room temperature and using a refractive index detector. Twenty microliters of each sample in Tetrahydrofuran (THF) (2% concentration) was filtered through 0.22 μm nylon filters and then injected. The separation columns were made of Phenogel (Phenomenex) and the mobile phase was THF (Scharlau TE 02252500). The calibration was performed with Poly Styrene (PS). The reproducibility of this measurement was better than 0.5%. Measurements were repeated three times to randomly selected specimens and deviations of the measured molecular weights were around ±600–700 g mol^{-1} in both cases.

Processability Measurements, Melt Flow Index. Melt flow indexes (MFI) were determined using a Tinius Olsen MP600 equipment at 190°C and 2.16 kg, for all the materials. The pellets were dried for 3 h at 80°C prior to the tests. The measurements were performed according to the ISO 1133:1997 standard, with a reproducibility of ±10%.

Thermal Degradation. The thermal stability was analyzed using a TA Instruments Q50 thermogravimetric analyzer. The measurements consisted of a heating ramp from room temperature to 600°C under inert atmosphere and from 600°C to 800°C under oxidative atmosphere, at a heating rate of 20°C min^{-1}. The reproducibility of the test is ±0.005 mg. To study the thermal degradation two parameters, T_{onset} and ΔT_d, were defined. T_{onset} is defined as the temperature at which 10% of the mass has been lost and ΔT_d is the temperature interval between T_{onset} and the temperature at which 90% of the mass has been lost. These parameters are considered to be suitable to describe the degradation related to the nanocomposite itself and during a noticeable loss of weight.

Microstructural Characterization. X-ray spectra of all samples were acquired using a Bruker D8 Advance Vário system, using Cu Kα radiation. The data were collected between 1° and 10° 2θ angles using a SoIX detector.

Transmission electron microscopy (TEM) images were recorded in a Philips CM120 Biofilter microscope, using an accelerating voltage of 120 kV. The samples were ultramicrotomed using a Leica Ultracut UCT cryo-ultramicrotome to 100 nm thickness slices.

RESULTS AND DISCUSSION

With the aim of establishing a reference for comparison, in the following subsections the results corresponding to the neat polymer will be presented and discussed first, and those obtained for the nanocomposites will follow.

Molecular Weight and Melt Flow Index Measurements

Poly(lactic acid). The molecular weight measurements of the processed PLA are shown on the top side of Table III. The molecular weight of the PLA pellets as received is 159,000 g mol^{-1}, which decreases with increasing extrusion screw speed during extrusion. Conversely, no significant effect on the molecular weight was found for varying injection moulding speeds. The poly-dispersity indexes (PDI) do not significantly change from one processing condition to another, meaning that the distribution of the polymer chain lengths remains similar.

These effects are confirmed by the melt flow index measurements. A value of 9 g 10 min^{-1} was measured for unprocessed PLA pellets, while the MFI for the PLA processed at 650 rpm and 120 mm s^{-1} was increased up to 19 g 10 min^{-1}. Clearly, the increase of extrusion screw speed and injection moulding speed increases the thermal and mechanical degradation as well. As the polymer was thoroughly dried according to the material specifications, hydrolysis was avoided. Therefore, PLA chains must mainly have degraded following random chain scission, and intermolecular and intramolecular transesterification reactions according to Carrasco et al., caused by temperature and mechanical forces during the transformation of the material.[20,21]

Table III. Molecular Weight, Melt Flow Index, and Thermal Stability Measurements for PLA and PLA/Clay Nanocomposites

	Extrusion speed (rpm)	Injection speed (mm s^{-1})	Molecular weight, M_w (g mol^{-1})	PDI	Melt flow index (g 10 min^{-1})	Degrad. factor, k_w	Degrad. temp., T_{onset} (°C)	Degrad. Interval, ΔT_d (°C)
INGEO 3051D	-	-	159,000	1.7	9	-	350	50
PLA	120	120	133,000	1.6	13	1.20	345	40
PLA	120	240	133,500	1.6	14	1.19	346	42
PLA	300	120	133,000	1.5	14	1.20	344	39
PLA	300	240	133,000	1.7	15	1.20	345	37
PLA	650	120	126,000	1.6	18	1.26	339	36
PLA	650	240	125,500	1.6	19	1.27	337	37
30B	120	120	125,000	1.5	17	1.28	346	53
30B	120	240	123,000	1.7	17	1.30	347	56
30B	300	120	122,500	1.7	20	1.30	351	59
30B	300	240	121,500	1.8	21	1.31	350	57
30B	650	120	119,000	1.7	24	1.34	351	56
30B	650	240	118,500	1.6	23	1.34	351	56
20A	120	120	126,000	1.9	25	1.26	354	45
20A	120	240	125,000	2.0	27	1.27	356	44
20A	300	120	119,500	1.7	26	1.33	353	49
20A	300	240	118,500	1.7	26	1.34	354	50
20A	650	120	112,500	1.7	46	1.41	353	50
20A	650	240	110,500	2.1	45	1.44	356	46

For the sake of an easier analysis of the molecular weight variations in the subsequent sections, a degradation factor has been defined as the ratio between the average molecular weight of the raw material and the average of molecular weight of processed polymer, k_w.[20]

PLA/Clay Nanocomposites. The final properties of the PLA/clay nanocomposites are not only influenced by processing parameters but also by the clay type and by its organomodification. Table III includes the GPC results of the nanocomposites. Overall, lower molecular weights were measured for the PLA/clay nanocomposites (e.g., 119,000 g mol^{-1} for 30B-650 rpm—120 mm s^{-1} and 112,500 g mol^{-1} for 20A-650 rpm—120 mm s^{-1}) as compared to the commercial pellets (159,000 g mol^{-1}) as well as to the processed PLA samples (125,500 g mol^{-1} for PLA—650 rpm—120 mm s^{-1}). Although the polymer matrix and clays were dried according to the specifications, clays absorb water rapidly and therefore the molecular weight reduction could be related to hydrolysis as well as to the thermal and mechanical degradation caused by the transformation.

Conversely, comparing the nanocomposites containing Cloisite 20A to the ones containing Cloisite 30B clay, it is noticeable that in general the molecular weight of the Cloisite 20A nanocomposites is lower than that of the corresponding Cloisite 30B nanocomposites.

This difference could result from the different degree of dispersion of the clays in the PLA matrix depending on the type of clay used (TEM images presented below in Figure 2, where the clay stacks are clearly smaller for the composite containing Cloisite 30B). Assuming a better dispersion implies a higher barrier effect, if the degradation during the extrusion is accelerated by the oxygen and/or the moisture trapped in the extruder, the composites with a better dispersion of the clays, that is, those containing Cloisite 30B, will undergo a milder degradation, whereas those containing 20A will degrade far more, as seems to be the case here.

As expected, also in the case of the nanocomposites increasing the screw speed during extrusion results in lower molecular weights. Conversely, varying the injection speed has no significant effect on the molecular weight of the samples. However, regarding the effect of the extrusion speed, it is noticed that k_w values increase from 1.28 up to 1.34 for the nanocomposites containing Cloisite 30B and from 1.26 to 1.44 for the ones containing Cloisite 20A.

Again, the melt flow index (MFI) results confirm the trends found for the molecular weight data. It is also noticed that the MFI for the nanocomposites containing Cloisite 20A is higher than for the neat PLA, for the same molecular weight (see Table III). According to the conclusions of Lewin et al., migration of clay platelets to the surface is likely to happen in the molten state, and cause lubrication.[31,32] Such migration of clay in the nanocomposite is governed by the interfacial tension between polymer macromolecules and clay platelets, and therefore it is more pronounced when the interactions between clays and polymer chains are weaker, as is the case for PLA and Cloisite 20A.

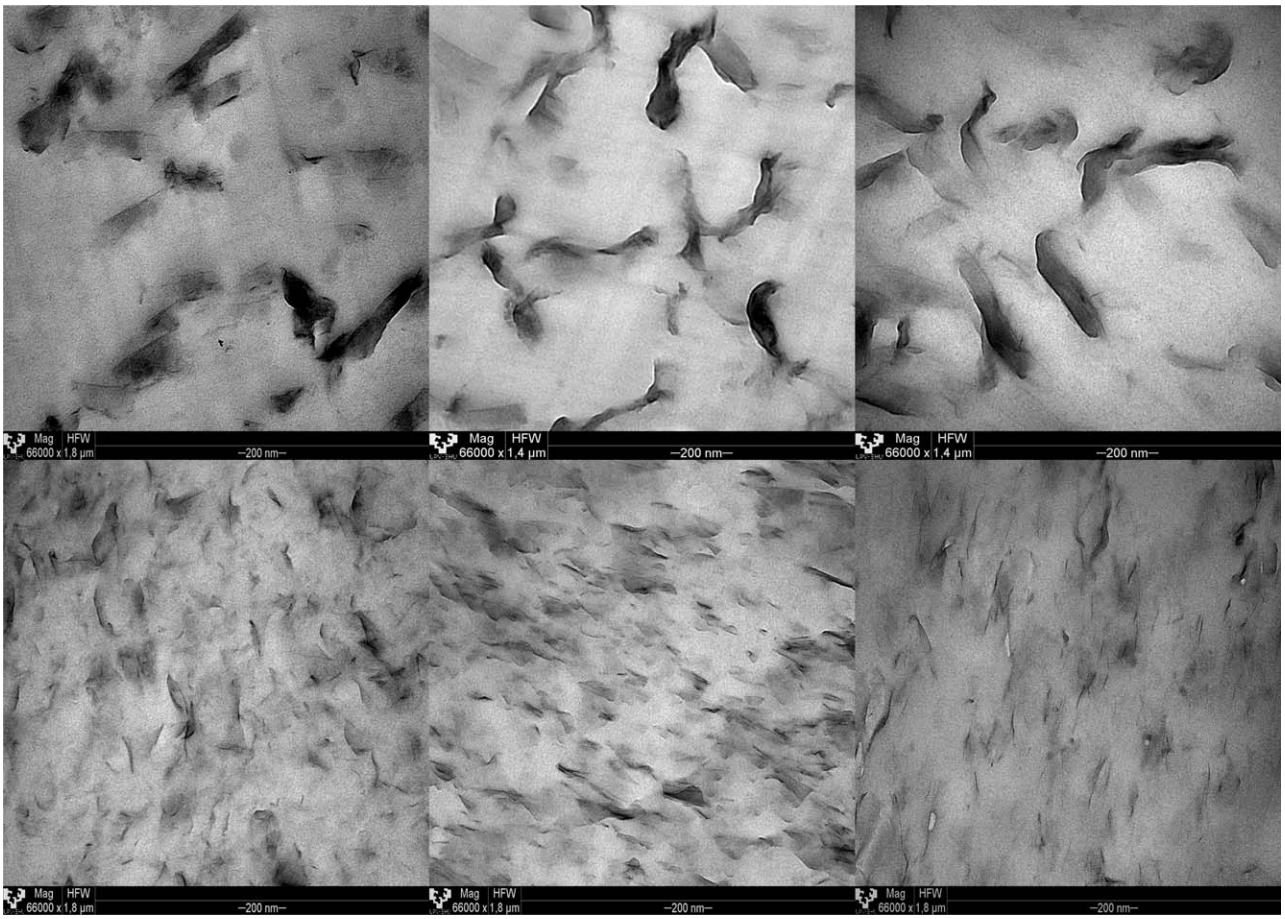

Figure 2. TEM micrographs for the PLA/Cloisite 20A (first row) and the PLA/Cloisite 30B (second row) nanocomposites, acquired from specimens obtained at several extrusion rates (120 rpm for the first column, 300 rpm for the second one, and 650rpm for the third one) and at 120 mm s^{-1} injection molding speed.

Considering the experimental error, for the only case in which a PLA sample and a Cloisite 30B nanocomposite have the same molecular weight (PLA extruded at 650 rpm and injected at 240 mm s^{-1} and the Cloisite 30B containing nanocomposite extruded at 120 rpm and injected at 120 mm s^{-1}) there seems not to be a significant difference in their MFI. Therefore, apparently the Cloisite 30B does not have the lubricating effect observed for the Cloisite 20A, certainly due to its better compatibility with the matrix.

Microstructural Characterization

The morphology of the samples obtained using various processing parameters and different clays was initially characterized on the injection moulded specimens by X-ray diffraction. As an example, the XRD spectra for Cloisite 30B and 20A organo-clays and their nanocomposites processed at 300 rpm and 120 mm s^{-1} are shown in Figure 1. The X-ray spectra of the organo-clays reveal a reflection peak at a 2θ angle of 4.88° for Cloisite 30B and another peak at a 2θ angle of 3.82° for Cloisite 20A, corresponding to basal spaces of 1.8 nm and 2.3 nm, respectively. The insertion of polymer chains inside clay galleries leads to an increase of the basal space d_{001} and hence, the corresponding diffraction peaks are shifted towards a lower diffraction angle for the nanocomposites ($2\theta = 2.8°$ for PLA/5 wt % Cloisite 30B and $2\theta = 2.7°$ for PLA/5 wt % Cloisite 20A, both extruded and injected in the same conditions; 300 rpm and 120 mm s^{-1}). Regardless of the clay type and processing conditions, all the nanocomposites show a reflection peak in between $2\theta = 2.9°$ (3 nm) and $2\theta = 2.7°$ (3.25 nm), indicating that complete exfoliation is not achieved by melt blending.

However, the diffraction patterns qualitatively differ for the nanocomposites depending of the type of clay they contain, as shown in Figure 1. The lower angle peak is sharper and more intense for the nanocomposite containing Cloisite 20A for which a second sharp and intense peak (compared to the ones shown by the nanocomposites containing Cloisite 30B) is also observed. This second peak may result from the d_{002} reflection or either from clay gallery collapsing, as has been reported before.[9] Gallery collapsing is more likely to occur when the affinity between the clay and the polymer is very low and therefore bigger tacktoids are formed. This is the case for the nanocomposites containing Cloisite 20A, as is shown in Figure 2.

To quantify the observed differences in morphology the Scherrer equation was used to estimate the sizes of the coherent diffraction domains, which correspond to the thickness of the clay stacks.[33,34] The results showed that for the nanocomposites containing Cloisite 20A the processing conditions had no effect on

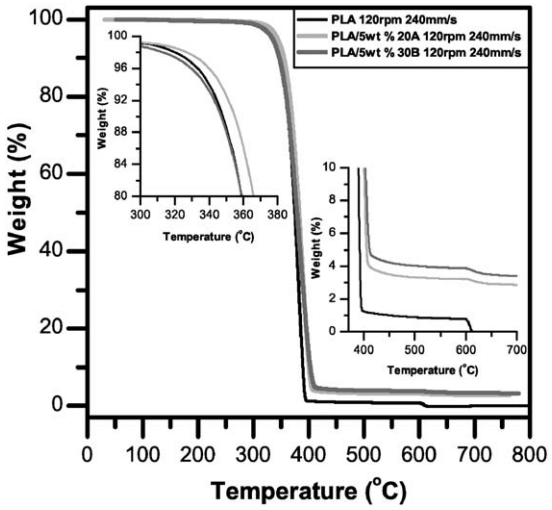

Figure 3. TGA results for PLA and PLA/clay nanocomposites extruded at 120 rpm and injection molded at 240 mm s^{-1}.

the size of the coherent diffraction domains, which were between 20 and 22 nm in every case. Conversely, for the nanocomposites containing Cloisite 30B the coherent domain sizes changed with the variation of extrusion speed from 25 nm (extruded at 120 rpm) to 15 nm (at 650 rpm) and to 8 nm (at 300 rpm). Besides, the injection moulding speed has no effect on the measured thickness for the clay stacks. Overall, according to the X-ray analysis the best dispersion of the clay appears to be obtained for PLA/5 wt % Closite 30B extruded at 300 rpm.

To assess those morphological differences between the nanocomposites via direct visualization, TEM was used to study the samples. In Figure 2, the TEM images for each of the nanocomposites injected at 120 mm s^{-1} are presented. Despite having very similar original dimensions, the TEM images of Figure 2 confirm that the Closite 30B clays are dispersed better than the Cloisite 20A ones. The higher affinity of the organomodification of the Cloisite 30B clays with the PLA is the cause for that difference. The TEM images and the X-ray results suggest that a mostly intercalated structure is obtained for the PLA/Closite 20A composites, while a partially exfoliated one is obtained for the PLA/Cloisite 30B nanocomposites.

Thermal Characterization

Poly(lactic acid). In this subsection, the stability of the processed materials as measured by TGA will be shown and discussed, taking into account the processing conditions each material has been subjected to. The onset temperature of the degradation reaction (T_{onset}) and the temperature interval to which it extends (ΔT_d) for each sample are shown in Table III, and some of the TGA curves are presented in Figure 3.

The TGA curves show that the PLA degradation occurs in a single step, where the entire polymer is degraded. For the neat PLA, it can be concluded that the more severe the processing conditions the lower the stability, both in terms of onset and degradation rate (see results in Table III). Taking into account that some of the degradation reactions undergone by PLA involve the polymer chain end-groups (unzipping and back-biting), and as for shorter chains the total amount of end-groups is larger, it is reasonable to state that observed lower stability of the final material is due to the decrease in molecular weight during processing, which has an accelerating effect on the degradation reactions.[21]

PLA/Clay Nanocomposites. As can be concluded from the TGA data in Table III and as illustrated in Figure 3, the thermal stability of PLA increases in presence of clays, resulting in higher onset temperatures and hindering the degradation reaction (increase of ΔT_d), in agreement with recent studies by Fukushima et al.[8] and Wei et al.[11] For instance, T_{onset} values increase from 344°C for PLA processed at 300 rpm and 120 mm s^{-1} to 351°C for the corresponding nanocomposite containing Cloisite 30B and up to 353°C for the PLA/Cloisite 20A one. In addition, for these same samples the thermal degradation for PLA occurs during a temperature interval of 42°C, while this interval increases to 49°C for the PLA/Cloisite 20A nanocomposite and up to 59°C for the nanocomposite containing Closite30B. The disparity between the residual inorganic weight (Figure 3) is due to the different amount of organic modification (Table I) that contains each type of clay.

To understand and compare the effect of the two clays, the microstructure must be taken into account. The better the distribution and higher the exfoliation degree, the higher the barrier effect originated by the high aspect ratio of the clays, as Carrasco el al.[20,21] and Najafi et al.[10] reported before. Moreover and according to a study by Cervantes-UC et al.[35] on the degradation of several commercial clays, the T_{onset} of Cloisite 30B is lower than that of Cloisite 20A due to the —OH radicals of the organomodification of Cloisite 30B, which are more susceptible to Hoffman reactions. However, a slowdown of the degradation (increase of the ΔT_d) is observed for the nanocomposites containing Cloisite 30B. Most probably, the higher barrier properties of the PLA/Cloisite 30B nanocomposite—as has been discussed in the previous section—delays the release of volatiles, slowing the degradation and thus increasing the ΔT_d values.

In that regard, it is noteworthy that the best dispersion of the clay is not obtained for the nanocomposites extruded at the highest speeds. Indeed, the PLA/Cloisite 30B nanocomposites extruded at 300 rpm are the ones for which the estimated size of the clay stacks was the smallest. The TGA measurements also suggest that these are the materials in which the barrier effect is most prominent as shown by their larger ΔT_d values, although admittedly the observed differences are not very significant.

One of the goals of this work is to establish an optimum combination of processing parameters that will result in nanocomposites having improved thermal stability, as compared to the neat PLA. As the number of parameters affecting the final result is large, an ANOVA analysis of the entire set of data was performed to evaluate the significance of the composition and processing parameters on the measured properties and to eventually reveal dependencies of the thermal stability on combinations of factors (processing conditions and composition) not considered so far. The results of the statistical analysis are shown in Table IV, where the *p*-values for the considered variables and combinations thereof are presented. The ANOVA test

Table IV. Statistical *p*-Values from ANOVA Analysis for Molecular Weight, Melt Flow Index, and Thermal Stability as a Function of Composition and Processing Parameters

	Clay	Extrusion	Injection	Clay: extrusion	Extrusion: injection	Clay: injection
M_w (g mol^{-1})	0.00001	0.00005	0.03	0.003	–	–
MFI (g 10 min^{-1})	0.000004	0.00002	–	0.0002	–	–
T_{onset} (°C)	0.0001	–	–	0.006	–	–
ΔT_d (°C)	0.0002	–	–	–	–	–

Only the *p*-values of the statistically significant variables are presented.

indicates which composition or processing parameter variations are statistically significant—that is, the observed relationship between the predictor and the response is not likely to be a result of chance—for each result according to the statistical parameter *p*.

p-values below a certain threshold (0.05 here) indicate that the variation of a certain parameter in study or interactions between several parameters are significant. Thus, from the data in Table IV it can be concluded that molecular weight and melt flow index are highly influenced by the type of clay and the extrusion speed. The interaction between the clay type and extrusion speed is also significant. As already mentioned before, the injection speed seems of less relative statistical significance, as the larger corresponding *p*-values (0.03) indicate. Regarding the degradation onset temperature and degradation temperature range, the obtained *p*-value is below 2×10^{-4} for the clay type. Hence, the thermal stability is mainly influenced by the addition of clays, and the type of clay used, and very little by the transformation parameters. This confirms what could be concluded from the results shown in Table III, where T_{onset} and ΔT_d clearly differ for each type of material, but not so much for different processing conditions and same clay type. As a consequence, there is no point in proposing a set of processing conditions that will minimize the thermal degradation, which was one of the goals of this work, but rather conclude that the use of clays alone will result in an improvement of the thermal stability of the material. Therefore, the optimum processing conditions must be defined attending to other properties.

In summary, the obtained results confirm the observations already discussed in previous sections and, more importantly, discard any other less obvious relation between the final properties and the processing conditions.

CONCLUSIONS

In this article, the degradation during processing and the thermal stability of PLA/clay nanocomposites as a function of the processing conditions has been studied. The novelty of this work as compared to previously existing similar investigations is the industrial nature of the used processing equipment and conditions. Also, one of the main goals was to determine an optimum combination of industrial processing conditions to maximize the thermal stability of the obtained end products.

Concerning the degradation during processing, it has been shown that the presence of the clays has a clear effect on the resulting molecular weights, which are consistently lower for the nanocomposites, most probably due to the hydrolysis induced by the water absorbed by the clays prior to processing. Moreover, the type of organomodification of the clay affects the extent of the degradation as well; the higher degree of dispersion of the Cloisite 30B clays seems to partially hinder the degradation.

The MFI data reveal that the lower compatibility of the Cloisite 20A with the PLA matrix results in a lubricating effect for these nanocomposites.

Regarding the microstructure, as expected the Cloisite 30B—because of their better compatibility with the matrix—is better dispersed than the Cloisite 20A ones. Moreover, the degree of dispersion of the Cloisite 20A is unaffected by the processing conditions. Thus, the type of organomodification of the clays is of such relevance that if a less compatible modification is chosen (such as the one used in the Cloisite 20A), the degree of dispersion drops dramatically and it cannot be appreciably increased by altering the processing conditions.

Conversely, when a more compatible organomodification is chosen (such as the one used in the Cloisite 30B), the processing conditions have a significant effect on the degree of dispersion and exfoliation of the clays. Moreover, it turns out that the degree of dispersion is not maximized by applying the most severe processing conditions (highest extrusion speeds here) but using somewhat milder conditions (300 rpm in this specific case). Speculatively, a variation of the extrusion rate could cause an alteration of the flow pattern inside the extruder resulting in a different mixing process inside the extruder. The decrease of the recorded torque of the extruder for the highest extrusion speeds would seem to support this hypothesis.

In any case, it has been clearly shown that the injection moulding step has almost no effect on any other analyzed parameters.

Finally, although for the neat PLA the degree of degradation during the processing appears to significantly affect its final thermal stability, such dependence is not observed for the nanocomposites, for which mainly the presence of clay and its type determine the degradation behavior. Indeed, the thermal stability of the composites is significantly higher than that of the neat material, but it appears that the effect of the processing conditions is almost negligible for the former. Thus, concerning T_{onset} and ΔT_d, there exists no clear optimum in processing conditions, and the definition of the most adequate processing

parameters will be based on other properties of the material. In this regard, the authors would like to point out that this work is part of a more comprehensive study in which the effect of the processing conditions on other relevant final properties (notably on the mechanical properties) will be assessed.

ACKNOWLEDGMENTS

Financial support from the Regional Government of Biscay (Dfb-6-12-TK-2010-25) is gratefully acknowledged. Maider Iturrondobeitia would like to thank the Government of the Basque Country for the scholarship *Ikertzaileak prestatzeko eta hobetzeko languntzak*. Technical and human support provided by Microscopy facilities at Biomedicine units as well as Microscopy Polymer Characterization unit of SGiker (UPV/EHU, MICINN, GV/EJ, ERDF, and ESF) is also gratefully acknowledged. Also, the authors would like to thank Jon Anakabe from Leartiker for his support in obtaining injection moulded specimens.

REFERENCES

1. Madhavan, N.; Nimisha Rajendran, N.; Rojan Pappy, J. *Bioresour. Technol.* **2010**, *101*, 8493.
2. Gupta, A. P.; Kumar, V. *Eur. Polym. J.* **2007**, *43*, 4053.
3. Ray, S. S.; Okamoto, M. *Prog. Polym. Sci.* **2003**, *28*, 1539.
4. Nieddu, E.; Mazzucco, L.; Gentile, P.; Benko, T.; Balbo, B.; Mandrile, R.; Ciardelli, G. *React. Funct. Polym.* **2009**, *69*, 371.
5. Henriette, M. C. *Food Res. Int.* **2009**, *42*, 1240.
6. Gámez-Pérez, J.; Nascimiento, L.; Bou, J. J.; Franco-Urquiza, E.; Santana, O. O.; Carrasco, F.; Maspoch, M. L. *J. Appl. Polym. Sci.* **2011**, *120*, 896.
7. Pavlidou, S.; Papaspyrides, C. D. *Prog. Polym. Sci.* **2008**, *33*, 119.
8. Fukushima, K.; Tabuani, D., Camino, G. *Mater. Sci. Eng. C.* **2012**, *32*, 1790.
9. Ojijo, V.; Ray, S. S. *Prog. Polym. Sci.* **2013**, *38*, 1543.
10. Najafi, N.; Heuzey, M. C.; Carreau, P. *J. Compos. Sci. Technol.* **2012**, *72*, 608.
11. Wei, P.; Bocchini, S.; Camino, G. *Eur. Polym. J.* **2013**, *40*, 932.
12. Zhu, J.; Wilkie, C. A. *Polym. Int.* **2000**, *49*, 1158.
13. Paul, M. A.; Alexandre, M.; Degée, P.; Henrist, C.; Rulmont, A.; Dubois, P. *Polymer* **2003**, *44*, 443.
14. Alamri, H. *Mater. Des.* **2012**, *42*, 214.
15. Kiliaris, P.; Papaspyrides, C. D. *Prog. Polym. Sci.* **2010**, *35*, 902.
16. Sothornvit, R.; Rhim, J. W. Hong, S. I. *J. Food Eng.* **2009**, *91*, 468.
17. Lasprilla, A. J. R.; Martinez, G. A. R.; Lunelli, B. H.; Jardini, A. L.; Filho, R. M. *Biotechnol. Adv.* **2012**, *30*, 321.
18. Lim, L. T.; Auras, R.; Rubino, M. *Prog. Polym. Sci.* **2008**, *33*, 820.
19. Zenkiewicz, M.; Richert, J.; Rytlewski, P.; Moraczewski, K.; Stepczynska, M.; Karasiewicz, T. *Polym. Test.* **2009**, *28*, 412.
20. Carrasco, F.; Pagés, P.; Gámez-Pérez, J.; Santana, O. O.; Maspoch, M. L. *Polym. Degrad. Stabil.* **2010**, *95*, 2508.
21. Carrasco, F.; Pagés, P.; Gámez-Pérez, J.; Santana, O. O.; Maspoch, M. L. *Polym. Degrad. Stabil.* **2010**, *95*, 116.
22. Auras, R.; Lim, L. T.; Selke, S. E. M.; Tsuji, H. Poly (lactic acid), Synthesis, Structures, Properties, Processing and Applications. Wiley: New York, **2010**.
23. Sin, T.; Rahmat, A. R.; Rahman, W. A. W. A. Polylactic Acid (PLA Biopolymer Technology and Applications). Elsevier Inc.: Oxford, United Kingdom, **2012**
24. McNeill, I. C.; Leiper, H. A. *Polym. Degrad. Stabil.* **1985**, *11*, 309.
25. Kopinke, F. D.; Remmler, M.; Mackenzie, K.; Moder, M.; Wachsen, O. *Polym. Degrad. Stabil.* **1996**, *53*, 329.
26. Carrasco, F.; Gámez-Pérez, J.; Santana, O. O.; Maspoch, M. L. *Chem. Eng. J.* **2011**, *178*, 451.
27. Saeidlou, S.; Huneault, M. A.; Li, H.; Park, C. A. *Prog. Polym. Sci.* **2012**, *37*, 1657.
28. Najafi, N.; Heuzey, M. C.; Carreau, P. J.; Wood-Adams, P. M. *Polym. Degrad. Stabil.* **2012**, *97*, 554.
29. Roy, P. K.; Hakkarainen, M.; Albertsson, A. C. *Polym. Degrad. Stabil.* **2012**, *97*, 1254.
30. Fischer, E.; Sterzel, H.; Wegner, G. *Colloid Polym. Sci.* **1973**, *251*, 980.
31. Lewin, M. *Fire Mater.* **2003**, *27*, 1.
32. Lewin, M. *Polym. Adv. Technol.* **2006**, *17*, 758.
33. Ray, S. S.; Okamoto, M. *Macromolecules* **2003**, *36*, 2355.
34. Causin, V.; Marega, C.; Marigo, A.; Ferrara, G. *Polymer* **2005**, *46*, 9533.
35. Cervantes, J. M.; Cauich-Rodríguez, J. V.; Vázquez-Tórres, H.; Garfias-Mesías, L. F.; Paul, D. R. *Therm. Termochim. Acta* **2007**, *457*, 92.